Numerical stress analysis in adhesive joints under thermo-mechanical load using model with special boundary conditions

IOP Conf. Series: Materials Science and Engineering **518** (2019) 032061 doi:10.1088/1757-899X/518/3/032061

Numerical stress analysis in adhesive joints under thermo-mechanical load using model with special boundary conditions

Nawres J. Al-Ramahi[1,2], Roberts Joffe[1,3] and Janis Varna[1]
[1]Division of Materials Science, Luleå University of Technology, SE-971 87 Luleå, Sweden.
[2]Institute of Technology / Baghdad, Middle Technical University, Baghdad, Iraq.
[3]Swerea SICOMP AB, Box 271, SE 941 26, Piteå, Sweden
E-mail: nawres.al-ramahi@ltu.se (Nawres J. Al-Ramahi)

Abstract. A numerical study of the adhesivejoint made of similar and dissimilar adherends subjected to thermo-mechanical loading is presented. A comprehensive numerical model was used for this purpose with the novel displacement coupling conditions which are able to correctly represent monoclinic materials (off-axis layers of composite laminates). The geometrical nonlinearity as well as nonlinear material model are also taken into account. Three different types of single-lap and double-lap adhesive joints are considered in this study: a) metal-metal; b) composite-composite; c) composite-metal. In case of composite laminates, four lay-ups are evaluated: uni-directional ([08]T and [908] T) and quasi-isotropic laminates ([0/45/90/-45]S and [90/45/0/-45]S). This paper focuses on the parameters which have the majoreffect on the peel and shear stress distribution within adhesive layer at the overlap ends. The comparison of behaviour of single-and double-lap joints in relation to these parameters is made. The master curves for maximum stress (peel and shear) at the ends of the overlap with respect to the bending stiffness and axial modulus of the adherends are constructed by analysing stress distributions in the middle of the adhesive.The main conclusions of this paper are: the maximum peel stress value for SLJ is reduced with increase of the adherend bending stiffness and for DLJ,similar behaviour was observed at the end next to the inner plate corner, while, at the end next to the outer plate corner peel stress is reduced with increase of adherend axial modulus.

1. Introduction

The fuel consumption in modern vehicles is one of the issues which have to be dealt with in order to reduce pollution emissions and exploitation costs.These goals can be achieved if the vehicle's weight is reduced by substitutionof some metal parts in structures by composites. However, while use of compositesensures reduction of weight, it should not affect safety of the vehicle (actually sometimesit can be even improved due to unique properties of composite materials). These considerations motivate most of the automotive and aerospace industries to employ composites in their structures [1], [2].Two most recent and well known examples from aircraft manufacturers are Boeing 787 and Airbus A380 [3]. The fuel consumption is decreasedby ~ 20% in the Boeing 787 due to use of composite material in structure (~50% by weight), similarly energy consumption is reduced by ~12% in Airbus A380 because 25% of weight of the structure is carbon fiber reinforced plastic (CFRP).In order to accommodate metals and polymer composites within one structure, the effective joining of parts is required. Thus, development of joints to connect similar and dissimilar materials is needed (e.g. composite-composite and composite-metal joints). There are three categoriesof joints that are typically considered: mechanical joint, adhesive joint or combination (hybrid) of both of them [4]. The adhesive joint has several advantages compared with other forms of joining [5], [6], [7].The most common type

of joint, due to its simplicity and effectiveness, is single-lap joint. Numerous studies are dedicated to the analysis of this type of joint. However, the stress state in single-lap joint is not most favorable because of inherent load eccentricity, causing misbalance and bending of the joint. Another most common type of joint is double-lap joint, since it is symmetric, it is generally considered to be better in terms of more uniform stress distribution. However, this advantage may not be as significant as it is thought of and it needs more comprehensive investigation. Therefor the current study presents the comparison between local stress distributions in the adhesive layer of single- and double- lap joints.

Numerous numerical and experimental studies have beenperformed on double-lap [8], [9], [10], 11] and single-lap [12–14] joints. However, often these investigations didnot consider thermal residual stresses which arise during the manufacturing of polymer composites and adhesive joints.

The adhesive joints arefrequentlycured at an elevated temperature and because of mismatch of thermal expansion coefficients for the joint members the residual thermal stresses arise when joint is cooled down to the temperature of use (e.g. room temperature). These stresses increasewith increase of the curing temperature for the adhesive. High thermal residual stresses may cause premature initiation of damage in joint which will result in catastrophic failure at rather low mechanical loads. Thus, thermal residual stresses must be included in the stress analysis of adhesive joints.

On the other hand, the composites are also manufacturedat elevated temperature and this will cause residual thermal stresses within the laminate itself (e.g. in plies with different fiber orientation in case of multi-axial laminate). These stresses sometimes cause the failure within the composite plate before any mechanical load is applied [15], which of course also means catastrophic failure of the joint and the whole structure.

There aresome attempts to account for residual thermal stresses for analysis of joint performance[16–21]. The effect of co-cured process on tensile load bearing capacity wasinvestigated experimentally and numerically for dissimilar (steel and composite adherend) DLJ in [16]. A 3D finite element model was used to combine thermal and mechanical load by means of linear superposition. The following parameters were taken in account: surface roughness; stacking sequence of the composite adherend; manufacturing pressure which is applied during the bonding process; contact area; adhesive thickness. The results showed that the tensile load bearing capacity of joint can be improved significantly by increasing the surface roughness for metallic adherend as well as by controlling the pressure during the manufacturing process.Another experimentally and numerically investigation for co-cured DLJ under tensile load with several design parameters was carried out in [17]. It was shown that increasing the fiber orientation in the $[\pm\theta]_{4S}$ stacking sequence results in decreasing the tensile load-bearing capacity.Experimental and numerical investigations of thermal residual as well as mechanical strains in DLJ (aluminum/aluminum and aluminum/carbon fiber-reinforced polymeradherends) werecarried out in [18]. The obtained results showed that more significant residual thermal stress is present in the adhesive layer in case of dissimilar compare to similar adherends. An experimental study for dissimilar adhesive joint (steel/CFRP) is presented in [19] to study the effect of the curing process on the joint efficiency under cyclic environmental loading (temperature and humidity). It was shown that the test conditions have a substantialeffect on the ultimate strength of the joint. The curing temperature didnot affect the ultimate joint strength if the test was done at room temperature but hada significant effect if the joint tested at elevated temperature.A 2D and 3D finite element models wereused in [20] to study the distribution of residual thermal stresses in SLJ and DLJ with similar and dissimilar adherends.The results showed that the geometrical and material non-linearity should be taken into account simultaneously in order to get accurate results. Moreover, the residual thermal stresses for the dissimilar adherendswerehigher than for similar adherends. Meanwhile, the residual thermal stresses (shear, longitudinal and transverse) for DLJ werehigher than for SLJ.The thermal stresses for DLJ with dissimilar adherends (aluminium/composite) was studied in [21]by using 3D finite element analysis.Two types of boundary conditions (constrained and free expansion concerning the width and length directions) were considered with four different type of composites adherends(boron/epoxy, graphite/epoxy, glass/epoxy and GLARE).It was shown that the higher thermal stresses are present for aluminium adherend in case of free expansion condition when the composite adherend (outer plate) had lower thermal expansion coefficient and higher longitudinal modulus in comparison toaluminium (inner plate). But in the case

of constraint conditions, theshear stress reducesin the composite corner and at the same time, it increasesin aluminium corner. While the peel stress (out-of-plane stress) slightly increasesat the aluminium corner and it changesfrom compression to tension at composite corner. Moreover, there was a significant increase in the in-plane normal stress components in length and width directions due to constraint conditions.

The objective of this paper is to study differences between the single and double-lap adhesive joints in terms of stress distributions and improve understanding of main parameters which influence the peel and shear stresses within the adhesive layer. Moreover, the influence of residual thermal stress on the peel and shear stress distributions as well as maximum values of these stresses areevaluated. In order to achieve these goals,special coupling boundary conditions developed in previous work [22] were employed in numerical model. The different scenariosto apply thermo-mechanical load were considered, similar to those described in [23].

2. Boundary condition and material properties

The stress analysis for DLJ and SLJ under mechanical load as well as thermo-mechanical loads wasdone by using the commercial finite element method (FEM) package ANSYS 19.2 (employing APDL codes).The geometry and dimensions for DLJ and SLJ are shown in Figure 1 and Figure 2 respectively.

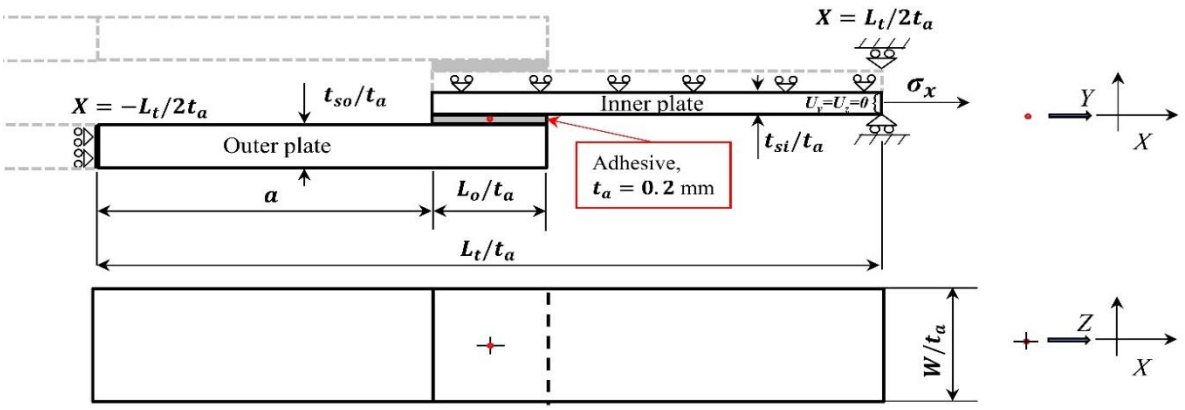

Figure 1. Geometry and dimensions of double-lap joint.

The 3D model used in this investigation has the following dimensions: adhesive thickness$t_a = 0.2\,mm$; overlap length/adhesive thickness ratio $L_o/t_a = 200$; total length/adhesive thickness ratio $L_t/t_a = 1500$; adherend/adhesive thickness ratio $t_s/t_a = 10$; and width/adhesive thickness ratio $W/t_a = 5$. All the geometrical parameters were normalized with respect to the adhesive thickness t_a thus results are valid for wide range of joints with different dimensions. In case when only mechanical load is applied on DLJ the load (as an average stress $\sigma_x = 120\,MPa$) was applied at the end of the inner plate (at $X = L_t/2t_a$ see Figure 1) along the length of the joint, whiledisplacements along the width and thickness ($U_y = U_z = 0$) were fixed. Moreover, the symmetry boundary condition was applied on the opposite end of the outer plate (at $X = -L_t/2t_a$) as well as on the top surface of the inner plate (at $Y = 0.5 \bullet t_a + t_{s1}/t_a$). Thus, only one-quarter of the whole model (see Figure 1) is used for the simulation, which results in fewer elements and shorter solution time. But in case of SLJ the symmetry boundary conditions are removed and fully clamped boundary condition is applied at one end (at $X = -L_t/2t_a$) with average stress ($\sigma_x = 60\,MPa$) applied at the opposite end at $X = L_t/2t_a$(see Figure 2).

In this investigation a novel boundary conditions are applied in order to separate the edge effects (at $X = \pm W/2t_a$) from the end effects (at $X = \pm L_o/2t_a$), essentiallythis is representation of an infinite plate; more details about these conditions are given in section 2.1.

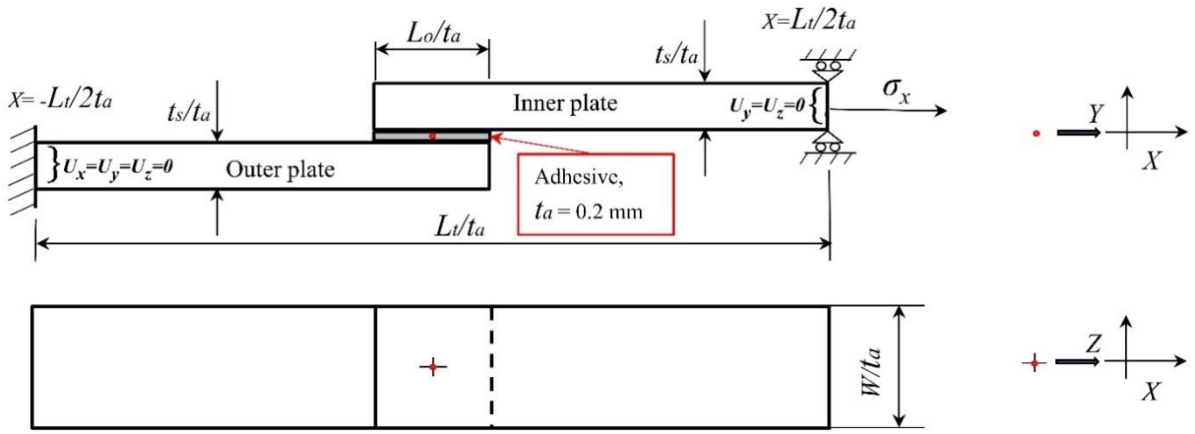

Figure 2. Geometry and dimensions of single-lap joint[22].

In order to prevent the interaction between ends of the joint (at $X = \pm L_t/2t_a$) and the overlap region, the load wasapplied a far away from the overlap ends ($X = \pm L_o/2t_a$). To ensure the accuracy of results as demonstrated in[20], [22], [24], the geometrical non-linearity option wasactivated in FEM. It should be noted that the geometrical non-linearity option will not affect the results in case of DLJ due to an absence of global bending and large local deformations but it was activated in order to have the same simulation options for DLJ and SLJ.

Table 1. Thermo-mechanical properties of adherends and adhesive materials.

CFRP unidirectional lamina (CF) [25]			
E_1 = 130 Gpa	G_{12} = 4.5 GPa	ν_{12} = 0.28	α_1 = -0.9×10^{-6} 1/K
E_2 = 8 GPa	G_{13} = 4.5 GPa	ν_{13} = 0.28	α_2 = 27×10^{-6} 1/K
E_3 = 8 Gpa		ν_{23} = 0.49	α_3 = 27×10^{-6} 1/K
GFRP unidirectional lamina (GF) [26]			
E_1 = 40 Gpa	G_{12} = 4 GPa	ν_{12} = 0.25	α_1 = 6×10^{-6} 1/K
E_2 = 8 GPa	G_{13} = 4 GPa	ν_{13} = 0.25	α_2 = 35×10^{-6} 1/K
E_3 = 8 GPa		ν_{23} = 0.45	α_3 = 35×10^{-6} 1/K
Aluminium _ linear (Al) [27]			
E_{Al} = 71 GPa		ν_{Al}= 0.33	α_{Al} = 23.1×10^{-6} 1/K
Adhesive _ linear (A) [27]			
E_{ad}= 2.7 GPa		ν_{ad} = 0.4	α_{ad} = 63×10^{-6} 1/K

1-fibresdirection.
2-transverse to the fibre's direction.
3-out-of-plane direction.
T-tangential.
The material notations used further in the text are given in brackets ().

Three different types of joint were considered in this study (the notations used: "M" – metal; "A" – adhesive; "C" – composite): a) metal-metal ([M/A/M]); b) composite-composite ([C/A/C]); c) metal-composite ([M/A/C]). In case of composite material, two types of polymer composites were used: glass fibre (GF) laminate ([GF/A/GF]); carbon fibre (CF) laminate ([CF/A/CF]), with four different stacking sequences $[0_8]_T$, $[90_8]_T$, $[0/45/90/-45]_S$ and $[90/45/0/-45]_S$.
The material properties along with notations used further in the text and graphs are given in Table 1 and Table 2 respectively (it should be noted that axial and bending stiffness of laminates are also presented in Table 2).

Table 2. Axial modulus and bending stiffness with notations for composite laminates.

Material	Stacking sequence	Notation		Mechanical properties	
		Text	graphs	E_x GPa	E_BN.m
CFRP	$[0/45/90/-45]_S$	CF-QI-0 (0-layer next to the adhesive layer)	CF_1	49.6	59
CFRP	$[90/45/0/-45]_S$	CF-QI-90 (90-layer next to the adhesive layer)	CF_2	49.6	21
CFRP	$[0_8]_T$	CF-UD-0	CF_3	130	87
CFRP	$[90_8]_T$	CF-UD-90	CF_4	8	5.3
GFRP	$[0/45/90/-45]_S$	GF-QI-0 (0-layer next to the adhesive layer)	GF_1	19.2	19
GFRP	$[90/45/0/-45]_S$	GF-QI-90 (90-layer next to the adhesive layer)	GF_2	19.2	9.6
GFRP	$[0_8]_T$	GF-UD-0	GF_3	40	27
GFRP	$[90_8]_T$	GF-UD-90	GF_4	8	5.4

E_B: bending stiffness.
E_x: axial modulus.

2.1. Coupling conditions

Special types of boundary conditions weredeveloped in order to prevent the stress concentration (due to finite width) at the edges ($at\ X = \pm W/2t_a$) to affect stress distribution within the adhesive layer.These conditions allow eliminating the width effect, in this case, a very narrow model can be used to simulate infinite plate with accurate results.This allows using a very fine mesh for the adhesive layer as well as the layers adjacent the adhesive, while only a couple elements are needed in width direction,whichdramatically shortens computation time. It should be mentioned that the boundary conditionsemployed here are different from the simple coupling which is often used in FEM simulations to enforce periodic structure. The boundary conditions in Figure 3 and Figure 4 can be used to simulate all material types(isotropic; orthotropic; as well as monoclinic composite layers with off-axis fibre orientations) with accurate results.

These boundary conditions were applied in two steps: a) first step, the coupling was applied on the all nodes within the vertical lines (through the thickness of the sample) at the edge A and B which have the same *X-coordinate*, this type of coupling forces selected nodes to have the same displacement $U_z$as shown in Figure 3; b) second step, the coupling was applied on the nodes through the width of the sample from ($Z = +W/2t_a$) to ($Z = -W/2t_a$). The selected nodes, in this case, should have the same *X-coordinate* and *Y-coordinate*. These nodes will be forced to have the same displacements U_x and U_y as shown in Figure 4. More details regarding these boundary conditions can be found in [22].

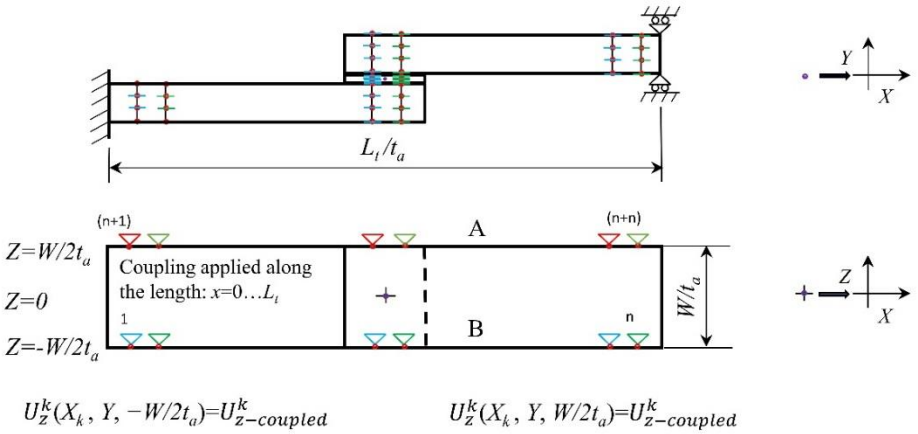

Figure 3. First set of coupling displacement U_z[28].

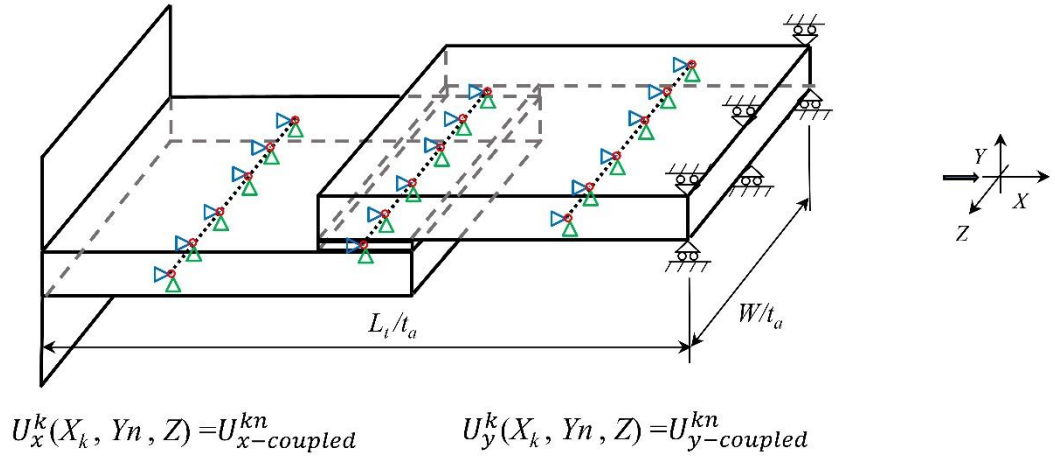

Figure 4. Second set of coupling displacement $U_x$and U_y[22].

2.2. Thermo-mechanical loading

To study the effect of thermal load on the stress distribution within the adhesive layer, the same strategy which is explained in [23]was used. Two types of joint manufacturing wereconsidered here: a)one-step curing; b) two-step curing. Depending on the manufacturing route the simulation has to be performed in two- or three- stages. In order to simulate [M/A/M] joint, two-stage simulation is required: 1) calculate thermal residual stresses (only temperature is applied); 2) application of the mechanical load. For this case, the residual thermal stresses werecalculated for the curing at 60^0C($\Delta T = -35^0$C is applied). But in case of simulating [C/A/C] or [M/A/C] there are two possible ways to perform calculations: I) two-stage simulation, this corresponds to the case when adhesive and composite adherend are cured simultaneously (co-curing), thus, the matrix of the composite also acts as an adhesive (the curing wasdone at 175^0C and $\Delta T = -150^0$C is applied);II) three-stage simulation, this is the case when the composite laminate wascured first and then joint wasassembled with different adhesive materialwhich wasalso cured ($\Delta T_1 = -115^0$Cwasapplied for the composite curingand $\Delta T_2 = -35^0$C wasapplied for the adhesive curing).TheFigure 5 shows the sequence of application of thermal and mechanical loads in form of the flowchart.

Further, in the figures, the following notations are used: (1S) - thermal load wasapplied once (curing of the adhesive only or adhesive and composite simultaneously); (2S) - thermal load wasapplied twice (first calculation for the thermal stresses in the composite and then in the whole joint).

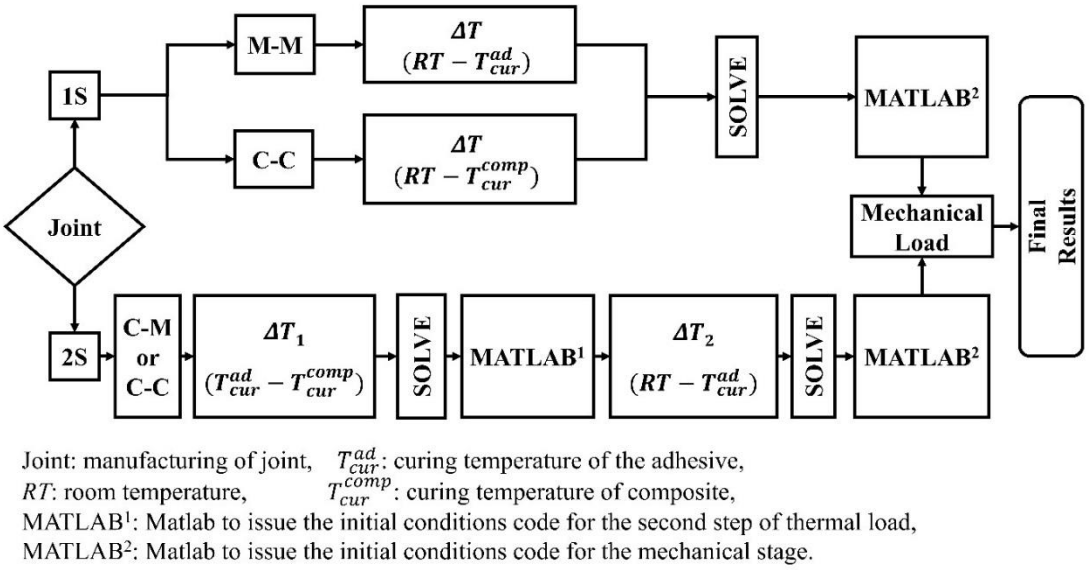

Joint: manufacturing of joint, T_{cur}^{ad}: curing temperature of the adhesive,
RT: room temperature, T_{cur}^{comp}: curing temperature of composite,
MATLAB[1]: Matlab to issue the initial conditions code for the second step of thermal load,
MATLAB[2]: Matlab to issue the initial conditions code for the mechanical stage.

Figure 5. Flowchart, represent the sequence of numerical simulation[29].

3. Results and discussion

In this section, the stress analysisis focused on the peel and shear stress distributionswithin adhesive layer, along the overlap length from ($X = -L_o/2t_a$) to ($X = L_o/2t_a$) at the centre of the adhesive layer.In order to study the differences in behaviour between the SLJ and DLJ, the obtained results are compared for similar and dissimilar adherends. Moreover, to study the effect of thermal residual stresses on the stress distribution within the adhesive layer, the results from mechanical loading only are compared with thermo-mechanical loading.In all cases (except dissimilar adherends) the SLJ has a symmetric stress distribution with respect to the line at $X = 0$ (half of the joint) because of that only half of the distribution is presented.

The trends for peel and shear stresses are completely different in case of SLJ or DLJ. For the DLJ the peel stressat the overlap end which is next to inner plate corner is always compressive. This means that it is a safer end in comparison with SLJ (compressive peel stresses in DLJ will not initiate failure). Moreover, for DLJ there is no symmetry in stress distribution with respect to the middle of adhesive.

3.1. Effect of adherend stiffness on stress distribution

Three different types of material wereused in this section in order to study the effect of adherend stiffness on the stress distribution within the adhesive layer: 1) isotropic material; 2) CFRP composite laminate; 3) GFRP composite laminate. Both adherends were considered of the same material.In case of an isotropic material, all the joint parameters werefixed and only the material stiffness was changed, three stiffness values wereused E = 140, 70 and 35 GPa (the aluminum Poisson's ratio wasused to calculate shear modulus). In case of anisotropic material (composite)the four different stacking sequences wereevaluated:CF-QI-0; CF-QI-90; CF-UD-0 and CF-UD-90.As shown in Figure6 for isotropic material, the adherend stiffness has a significant effect on the peel and shear stress distribution in the adhesive layer. The peel and shear stress concentration are reduced with the increase of the adherend stiffness in both cases with more significant effect for DLJ than SLJ, as well as the stress perturbation zone is increased with the increase of the stiffness. On the other hand the peel stress concentration for DLJ is lower than for the SLJ with larger perturbation zone, while higher shear stress concentration with lower plateau region is obtained for DLJ.

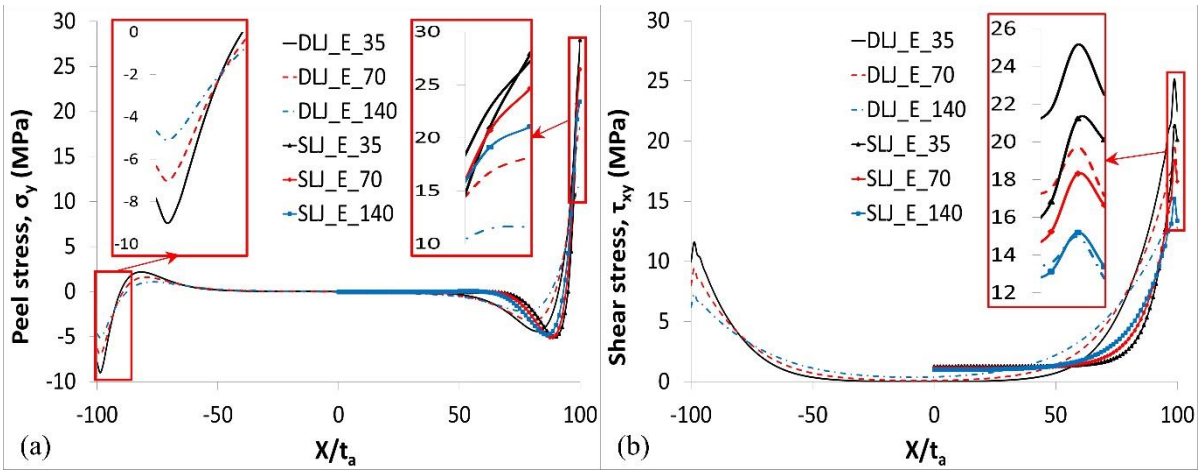

Figure 6. The effect of changing the adherend stiffness on peel (a) and shear (b) stress distributions in adhesive layer for [M/A/M] SLJ and DLJ, $t_a = 0.2\ mm$, $t_s/t_a = 10$,$L_o/t_a = 200$.

In case of composite adherends,as shown in Figure 7, the maximum peel and shear stress concentration is obtained for CF-UD-90 which has the lowest stiffness, but the minimum peel and shear stress concentration is observed for CF-UD-0 which is the stiffest laminate. This behaviour is similarto the trends observed for isotropic material. The highest peel and stress concentration at the end of overlap in DLJ is found when the adherends have low stiffness, while with the high adherend stiffness in the DLJ the lowest peel and shear stress concentration level at overlap end is observed in comparison with SLJ.Moreover, if quasi-isotropic laminate is considered the peel and shear stress concentration have approximately the same value for SLJ and DLJ.

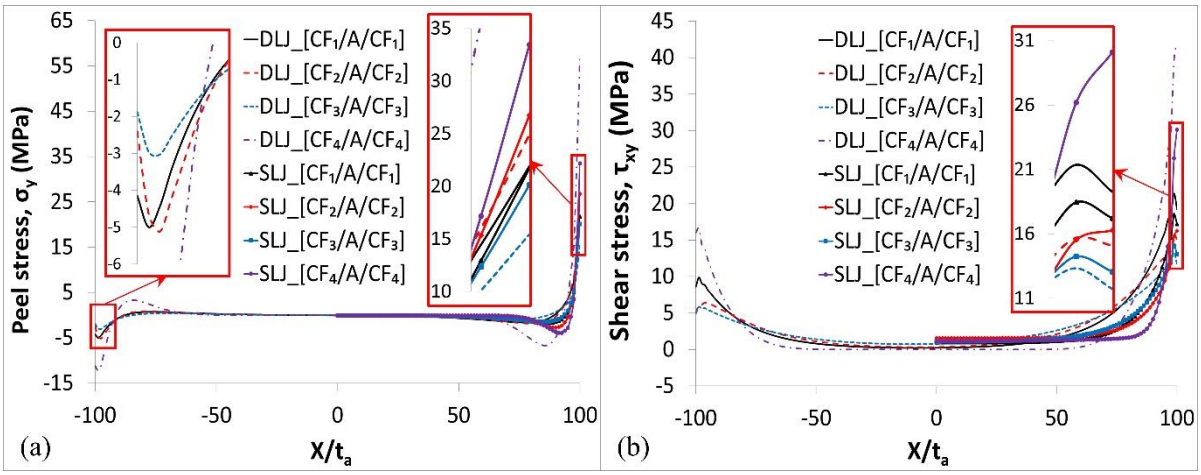

Figure 7. Comparison of peel (a) and shear (b) stress distributions in the adhesive layer of [CF/A/CF]SLJ and DLJ with different stacking sequence of plies,$t_a = 0.2\ mm$, $t_s/t_a = 10$,$L_o/t_a = 200$.

In this part the comparison wasmadebetween the aluminium, CF-QI-0 and GF-QI-0. The axial modulus of adherend materials were (71, 49.6 and 19.2) for aluminium, CF-QI-0 and GF-QI-0 respectively. According to the previous conclusion, theranking of maximum peel stress at the end of the overlap should be the following: Al, CF and GF and it is satisfied for DLJ at ($X = L_o/2t_a$)as can be seen in Figure8. Howeverin case of SLJ as well as the DLJ at ($X = -L_o/2t_a$), different behaviour is obtained: peel stress in Al is between stress levels in CF and GF composites. Meanwhile the previous conclusions hold the same for the shear stress component. It means that there is other than stiffness

parameter whichaffects the maximum peel stress for SLJ and DLJ at the end next to inner plate corner. This behaviour is compatible with findings in [22]: the maximum peel stress depends on the bending stiffness of the plate and it follows the same trend (see Table 2 for values of bending stiffness).

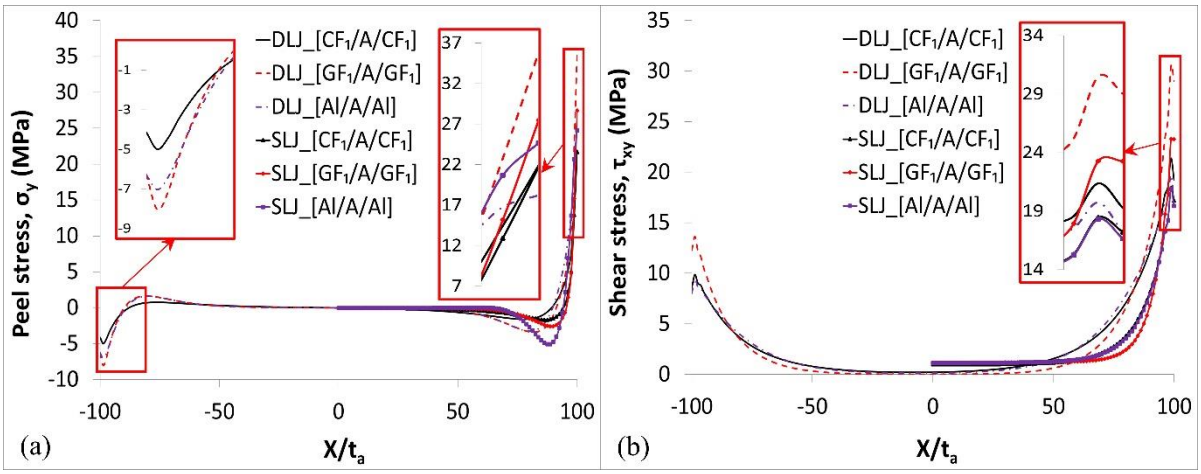

Figure 8. Comparison of peel (a) and shear (b) stress distributions in adhesive for SLJ and DLJ with different adherends material,$t_a = 0.2\ mm$, $t_s/t_a = 10$,$L_o/t_a = 200$.

3.2. Effect of the adherendthickness

In this section,threedifferent adherend thicknesses were considered to study effect of this parameter on peel and shear stress distribution. In the first part,the same thickness for both adherends was used ($t_s/t_a = 10$and $t_s/t_a = 20$) as shown in Figure9.

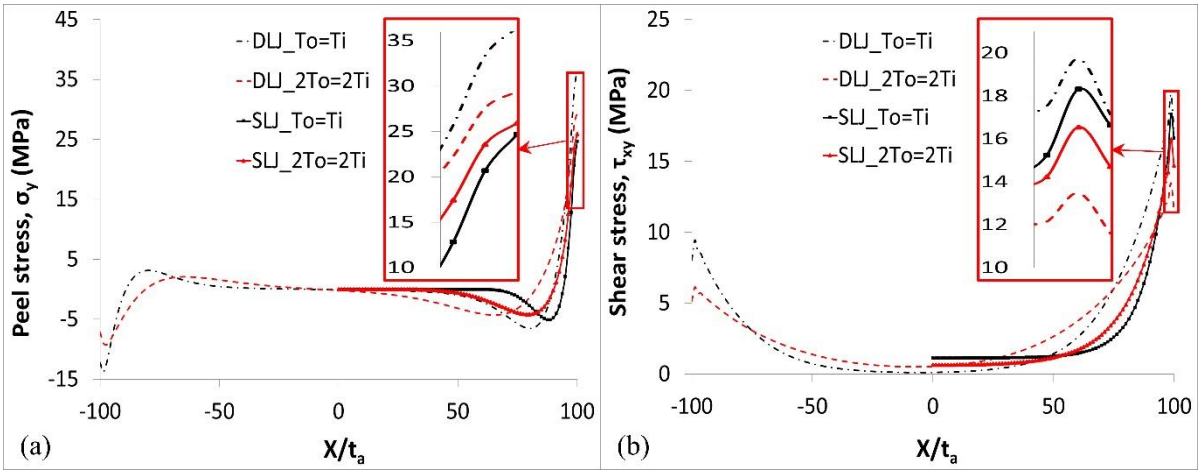

Figure 9. Comparison of peel (a) and shear (b) stress distributions for two different adherend thickness. For DLJ and SLJ with [Al/A/Al], $t_a = 0.2\ mm$,$L_o/t_a = 200$.

In the second part, one of the adherend was kept the same but the other was changed as shown in Figure 10 and Figure 11. In order to prevent change of the force as the cross-section area was changed, the force (120 N) was applied instead of average stress. The Al was considered to be adherend material. Regarding the case when both adherends have the same thickness (see Figure 9), the results show that for DLJ the peel stress concentration reduces at both ends with increase of the adherend thickness, which may be due to the increase of the bending stiffness of the adherend plate. The stress perturbation zone is increased with increasing the adherend thickness. On the other hand, the shear stress concentration at the ends of the overlap is reduced with increase of the adherend thickness, as

well as the plateau region is reduced and the level of it is increased, which is likely due to the reduction of the σ_x. But in case of SLJ the peel stress concentration and stress perturbation zone are increased with increasing the adherend thickness, moreover, the shear stress concentration is reduced with increase of the adherend thickness; the plateau level is also reduced and the length of the plateau becomes shorter.

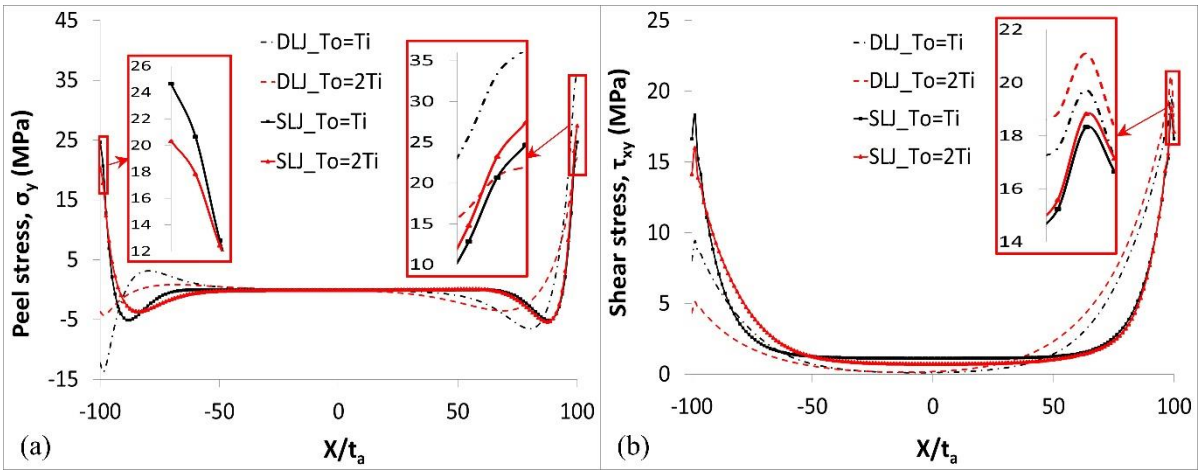

Figure 10. Comparison of peel (a) and shear (b) stress distributions for adherends with the same thickness ratio ($t_s/t_a = 10$) and for the outer plate thickness with the adjusted ratio ($t_s/t_a = 20$). For DLJ and SLJ with [Al/A/Al], $t_a = 0.2\ mm$, $L_o/t_a = 200$.

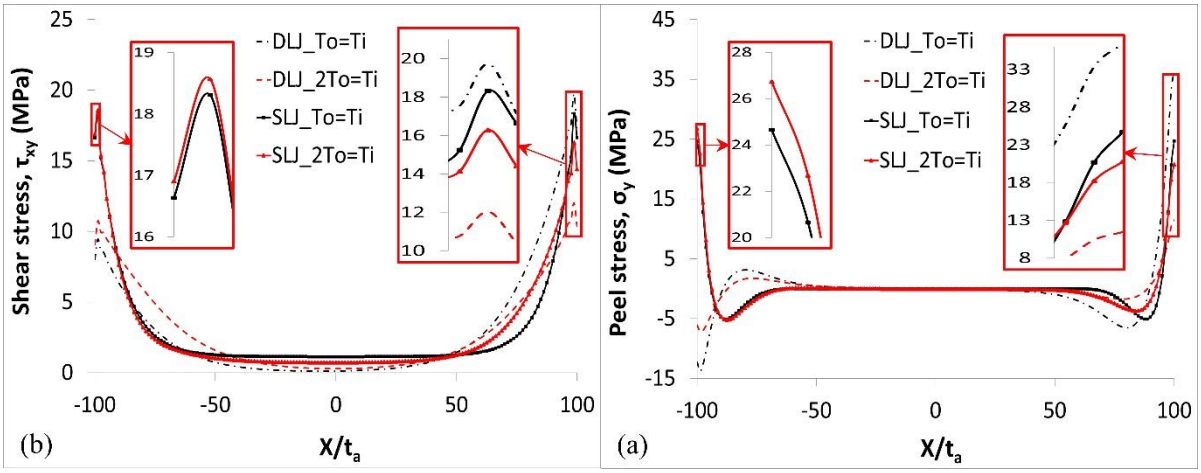

Figure 11. Comparison of peel (a) and shear (b) stress distributions for adherends with the same thickness ratio ($t_s/t_a = 10$) and for the inner plate thickness with the adjusted ratio ($t_s/t_a = 20$). For DLJ and SLJ with [Al/A/Al], $t_a = 0.2\ mm$, $L_o/t_a = 200$.

In case of the DLJ increasing the thickness of one adherend plate while keeping the second adherend plate constant show the following results: thickness increase of outer or inner plate causes reduction of the stress concentration at the end of the overlap, with more significant effect when increasing the inner plate thickness two times (see Figure 10 and Figure 11). But in case of SLJ, the peel stress concentration increased at the overlapping end which is next to the corner of the thicker plate and reduced on the other end. Also, the shear stress concentration for DLJ and SLJ increased at the overlapping end which is set next to thicker plate corner and it reduced at the other end.

3.3. The effect of manufacturing process on stress distribution

In order to evaluate the effect of residual thermal stress on peel and shear stress distribution, the stress results under mechanical load only (OM) werecompared with thermo-mechanical loading. Three types of DLJ and SLJ wereconsidered in this section: [Al/A/Al], [CF/A/CF] and [CF/A/Al].In both cases (DLJ and SLJ) the peel and shear stress distribution have the same trend, but with lower maximum stress at the ends of the overlapping for thermo-mechanical load. In case ofisotropic material (Al), only one-step of curing is presented, the peel stress for DLJ reduced by ~20% at ($X = L_o/2t_a$) and by ~50% at ($X = -L_o/2t_a$) as well as for SLJ reduced by ~10% due to thermal load, but with approximately the same maximum shear stress value, as shown in Figure12.In case of CF (a quasi-isotropic stacking sequence with 0-layer adjacent to adhesive layer) two types of manufacturing (one-step of curing and two-step of curing) are presented and compared with OM case as shown in Figure13. The peel stress concentration is reduced in both cases (DLJ and SLJ) due to residual thermal stress with a more significant effect for one-step curing.The maximum peel stress for SLJ reduces more than for DLJ at ($X = L_o/2t_a$),while the DLJ show increase in peel stress approximately 3 times at ($X = -L_o/2t_a$). Theseresults show that the manufacturing of joint in one-step gives the lowest value of peel and shear stress concentration at the ends of overlap. Therefore, only one-step curing was considered for comparison between the peel and shear stress distribution with a different stacking sequence of plies in adherends.

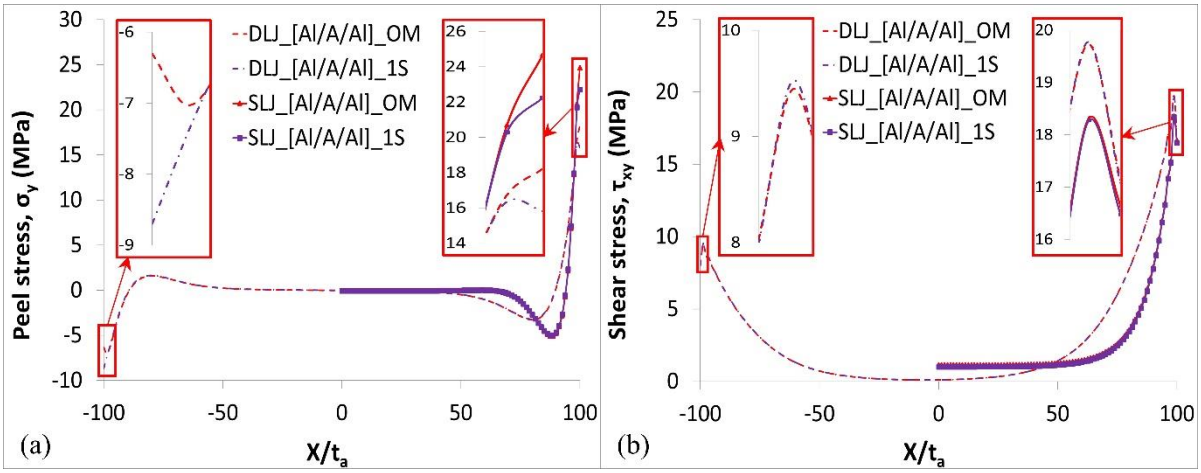

Figure 12. The comparison of peel (a) and shear (b) stress distributions in the adhesive layer of [Al/A/Al] DLJ and SLJ with and without residual thermal stresses accounted for, 120MPa and 60 MPa for DLJ and SLJ respectively and $\Delta T = -35^0$C are applied.

In order to investigate the effect of residual thermal stress on the stress distribution (e.g. the maximum peel and shear stress at the overlap ends) of different composite stacking sequence, the comparison of four different stacking sequences was performed. This was done in the same way as described section 3.1. The maximum and minimum peel and shear stresses are observed for DLJ with 90-layer and 0-layer respectively as can be seen in Figure 14. These results also show that the peel and shear stress concentration at the overlap ends are shifted down with approximately the same value in both cases, SLJ or DLJ (the comparison wasdone between Figure 7 and Figure 14). In case ifthermal stresses weretaken into account, the peel stress concentration is reduced as follows (the relative difference in stress values between simulations with and without thermal stresses is presented): 1) in case of SLJ with CF-QI-90 by ~90%, CF-UD-0 by 65%, CF-QI-0 by ~60%, CF-UD-90 by 40%; 2) in case of DLJ with CF-QI-90 by ~90%, CF-UD-0 by 80%, CF-QI-0 by ~55%, CF-UD-90 by 25%. The abovementioned means that the peel stress can be significantly reduced by swapping 0-layer by 90-layer in the quasi-isotropic laminate. Moreover, for DLJ the stiffer laminate (CF-UD-0) causes larger reduction than for the SLJ, while for SLJ the softer laminate (CF-UD-90) causeseven more significant decrease than for the DLJ. On the other hand as a result of these differencesin the reduction of

maximum peel and shear stress, the valuesof stresses in these laminate will differ also in case when only mechanical load is applied.

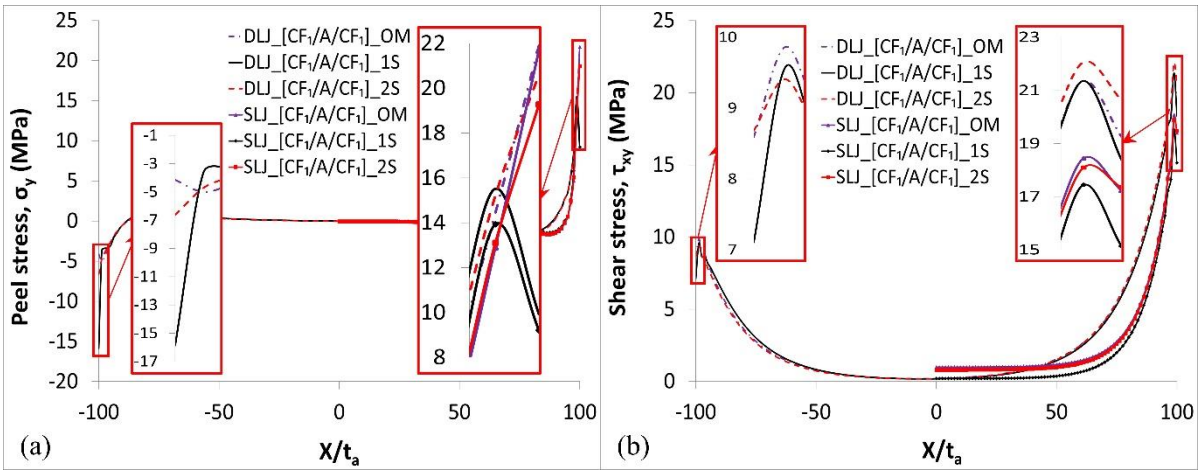

Figure 13. The comparison of peel (a) and shear (b) stress distributions in the adhesive layer of [CF_1/A/CF_1] DLJ and SLJ with and without residual thermal stresses accounted for, 120MPa and 60 MPa for DLJ and SLJ respectively, $\Delta T = -150^0$C for one-step curing and $\Delta T = -35^0$C for two-step curing are applied.

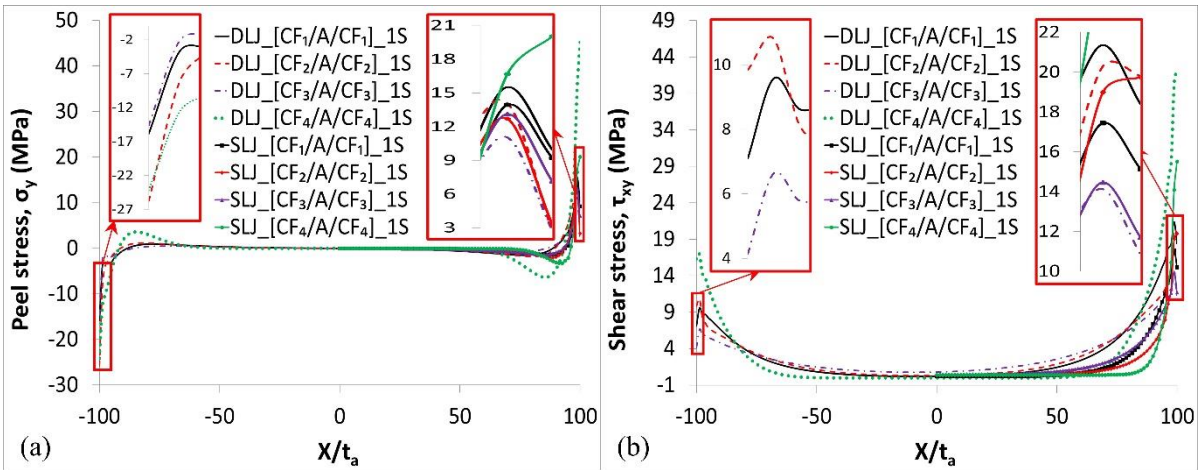

Figure 14. The comparison of peel (a) and shear (b) stress distributions in the adhesive layer of [CF/A/CF] DLJ and SLJ with different stacking sequence of plies in adherends, 120MPa and 60 MPa for DLJ and SLJ respectively, $\Delta T = -150^0$C for one-step curing are applied.

Two types of materials were used as adherend material, isotropic material (Al) and anisotropic material (CF-QI-0).In this case the SLJ has also unsymmetrical peel and shear stress distributions, because of that full curves are presented.The peel stress concentration is reduced significantly in both cases (DLJ and SLJ) at both ends when residual thermal stress was accounted for.Moreover, the peel stress for DLJ and SLJ move to compressive stress at ($X = L_o/2t_a$) which is next to composite corner (outer plate corner) with a very high compressive stress value and with longer perturbation zone for DLJ as shown in Figure15. This means that a very safe adhesive joint can be constructed by using DLJ with dissimilar adherends.

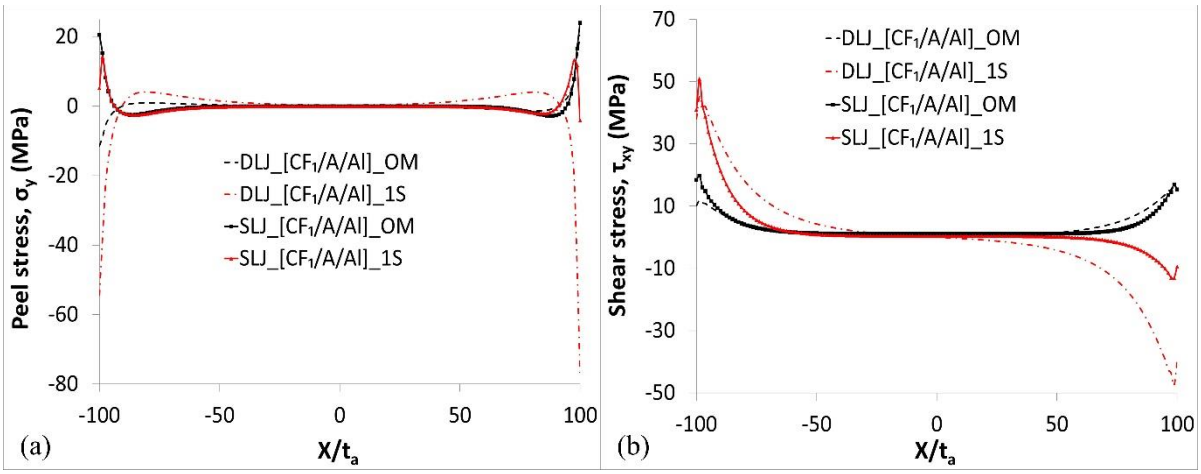

Figure 15. The comparison of peel (a) and shear (b) stress distributions in the adhesive layer of [CF_1/A/Al] DLJ and SLJ with and without residual thermal stresses accounted for, 120MPa and 60 MPa for DLJ and SLJ respectively, $\Delta T = -150^0$C for one-step curing are applied.

3.4. Comparison of master curves in case if thermal stresses are accounted for

In the previous sections the peel and shear stress distributions were investigated in the adhesive layer for different adherend material as well as different laminate lay-ups. The analysis of the results shows that there are two parameters which have the major effect on the maximum of peel and shear stress. These parameters are adherend bending stiffness for maximum peel stress and adherend axial modulus for maximum shear stress.The adherend bending stiffness which is given in Table 2,is presented versus the maximum peel stress in Figure16a. Figure 16 shows that the maximum peel stress value reduces with increasing the bending stiffness of the adherend. This finding is satisfied for SLJ at both ends as demonstrated in [22]. But for DLJ it is valid at the end which is next to the inner plate corner but the stress at the second end which is next to the outer plate corner dependents on the axial modulus of adherend. The curing in one-step and two-step have the same effect on the stress level (the trend is the same as can be seen in Figure 16a), but with lower maximum peel stress value when the joint was manufactured in one-step. The DLJ curves mirror SLJ curves with higher shift between one-step and two-step curves. The maximum shear stress is presented vs the adherend axial modulus (given in Table 2) in Figure 16b. The maximum shear stress is reduced with increasing adherend axial modulus, but the behaviour is slightly different between the DLJ and SLJ.

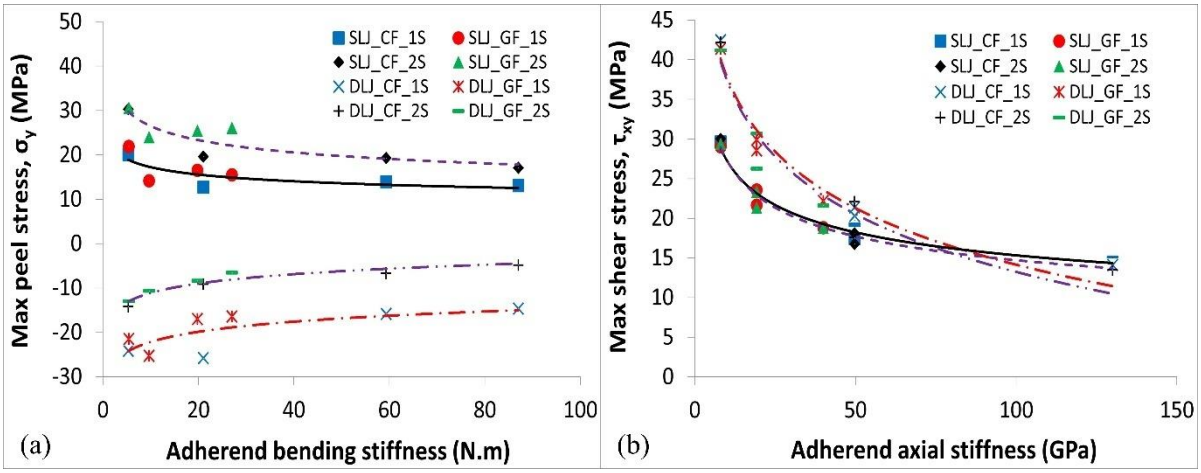

Figure 16. Maximum peel (a) and shear (b) stress under thermos-mechanical load in the adhesive with respect to bending stiffness and axial modulus respectively for DLJ and SLJ.

4. Conclusions

The analysis of stress distributions in the adhesive layer of various types of SLJ and DLJ manufactured with different assembly strategies led to the following conclusion:

1- The increase of thickness of all adherendsdifferently affects peel stress concentration for DLJ and SLJ: it is reduced for DLJ but increased for SLJ. Meanwhile, the shear stress concentration is reduced in both types of joints.
2- Increase of the thickness either of inner or outer adherend platewhile keeping the other adherend the same causes a reduction of the peel stress concentration at the overlap ends of DLJ. In case of SLJ, the increase of thickness of one of the adherend causes an increase in the peel stress concentration at the overlap end next to the corner of the thicker plate but it is reduced on the other end.
3- The shear stress concentration for DLJ and SLJ is increased at the overlap end next to thicker plate corner but it is reduced at the other end due to the increase of thickness of inner or outer adherend plate.
4- The manufacturing of adhesive joint in one-step results in lowest value of peel and shear stress concentration at the ends of overlap.
5- In case of the quasi-isotropic laminate adherend, the strength of SLJ and DLJ can be significantly improved by using 90-layer adjacent to the adhesive layer (instead of 0-layer).
6- The minimum peel stress concentrations for SLJ can be achieved by using dissimilar adherends. Moreover, in case of DLJ the peel stress concentration is compressive.
7- For SLJ the maximum peel stress value is reduced with increase of the adherend bending stiffness. Similarly it is reduced for DLJ at the end next to the inner plate corner.However, at the end next to the outer plate corner it is reduced with increase of adherend axial modulus.
8- The maximum shear stress value is reduced with increase the adherend axial modulus for both, SLJ and DLJ.

References

[1] Kweon J-H, Jung J-W, Kim T-H, Choi J-H and Kim D-H 2006 Failure of carbon composite-to-aluminum joints with combined mechanical fastening and adhesive bonding *Compos. Struct.***75** 192–8
[2] Khashaba U A, Sallam H E M, Al-Shorbagy A E and Seif M A 2006 Effect of washer size and tightening torque on the performance of bolted joints in composite structures *Compos. Struct.***73** 310–7
[3] Li X, Guan Z, Li Z and Liu L 2014 A new stress-based multi-scale failure criterion of composites and its validation in open hole tension tests *Chinese J. Aeronaut.***27** 1430–41
[4] Puchała K, Szymczyk E and Jachimowicz J 2012 About mechanical joints design in metal-composite structure *J. KONES***19** 381–90
[5] Wahab M M A 2012 Fatigue in adhesively bonded joints: a review *ISRN Mater. Sci.*
[6] Kim K-S, Yi Y-M, Cho G-R and Kim C-G 2008 Failure prediction and strength improvement of uni-directional composite single lap bonded joints *Compos. Struct.***82** 513–20
[7] Pramanik A, Basak A K, Dong Y, Sarker P K, Uddin M S, Littlefair G, Dixit A R and Chattopadhyaya S 2017 Joining of carbon fibre reinforced polymer (CFRP) composites and aluminium alloys-A review *Compos. Part A Appl. Sci. Manuf.***101** 1–29
[8] Santos T F and Campilho R D S G 2017 Numerical modelling of adhesively-bonded double-lap joints by the eXtended Finite Element Method *Finite Elem. Anal. Des.***133** 1–9
[9] Amidi S and Wang J 2018 An analytical model for interfacial stresses in double-lap bonded joints *J. Adhes.***8464** 1–25.
[10] Sülü İ Y 2018 Mechanical behavior of composite parts adhesively jointed with the insert double-lap joint under tensile load *Weld. World***62** 403–13.
[11] Mokhtari M, Madani K, Belhouari M, Touzain S, Feaugas X and Ratwani M 2013 Effects of composite adherend properties on stresses in double lap bonded joints *Mater. Des.***44** 633–9.
[12] Grant L D R, Adams R D and da Silva L F M 2009 Experimental and numerical analysis of single-lap joints for the automotive industry *Int. J. Adhes. Adhes.***29** 405–13.

[13] Broughton W R and Hinopoulos G 1999 *Evaluation of the single-lap joint using finite element analysis* (National Physical Laboratory. Great Britain, Centre for Materials Measurement and Technology)
[14] Y Yang L Wu Y G Z Z 2011 Effect of adherent thickness on strength of single-lap adhesive composites joints *Int. Conf. Heterog. Mater. Mech.* 679–682.
[15] Hahn H T 1976 Residual stresses in polymer matrix composite laminates *J. Compos. Mater.***10** 266–78.
[16] Shin K C and Lee J J 2003 Bond parameters to improve tensile load bearing capacities of co-cured single and double lap joints with steel and carbon fiber-epoxy composite adherends *J. Compos. Mater.***37** 401–20.
[17] Shin K C and Lee J J 2000 Tensile load-bearing capacity of co-cured double lap joints *J. Adhes. Sci. Technol.***14** 1539–56.
[18] Jumbo F, Ruiz P D, Yu Y, Swallowe G M, Ashcroft I A and Huntley J M 2007 Experimental and numerical investigation of mechanical and thermal residual strains in adhesively bonded joints *Strain***43** 319–31.
[19] Nguyen T-C, Bai Y, Zhao X-L and Al-Mahaidi R 2013 Curing effects on steel/CFRP double strap joints under combined mechanical load, temperature and humidity *Constr. Build. Mater.***40** 899–907.
[20] Jumbo F S, Ashcroft I A, Crocombe A D and Wahab M M A 2010 Thermal residual stress analysis of epoxy bi-material laminates and bonded joints *Int. J. Adhes. Adhes.***30** 523–38
[21] Rastogi N, Soni S R and Nagar A 1998 Thermal stresses in aluminum-to-composite double-lap bonded joints *Adv. Eng. Softw.***29** 273–81.
[22] Al-Ramahi N J, Joffe R and Varna J 2018 Investigation of end and edge effects on results of numerical simulation of single lap adhesive joint with non-linear materials *Int. J. Adhes. Adhes.***87** 191–204.
[23] Al-Ramahi N 2018 *Numerical stress analysis in hybrid adhesive joint with non-linear materials*Licentiate thesis(Luleå University of Technology,ISBN: 978-91-7790-034-4)
[24] Apalak M K and Gunes R 2002 On non-linear thermal stresses in an adhesively bonded single lap joint *Comput. Struct.***80** 85–98.
[25] Shin K C and Lee J J 2006 Effects of thermal residual stresses on failure of co-cured lap joints with steel and carbon fiber–epoxy composite adherends under static and fatigue tensile loads *Compos. Part A Appl. Sci. Manuf.***37** 476–87.
[26] Mechanical properties of glass fiber reinforced polymer unidirectional lamina. These material properties from the website of Performance Composites Limited company. URL ⟨http://www.performance-composites.com/carbonfibre/mechanicalproperties_2.asp⟩.
[27] Wahab M A 2014 *The Mechanics of Adhesives in Composite and Metal Joints: Finite Element Analysis with ANSYS* (DEStech Publications, Inc).
[28] Al-Ramahi N, Joffe R and Varna J 2018 FEM analysis of stresses in adhesive single-lap joints with non-linear materials under thermo-mechanical loading *ECCM18-18th European Conference on Composite Materials Athens, Greece, 24-28th June 2018.*
[29] Al-Ramahi N J, Joffe R and Varna J 2018 Numerical stress analysis in adhesively bonded joints with non-linear materials under thermo-mechanical loading *Eng. Struct.*

Acknowledgement
The research leading to these results was financially supported by Middle Technical University (Baghdad, Iraq), by Polymeric Composite Materials group at Luleå University of Technology (Luleå, Sweden) and by the strategic innovation programme LIGHTer provided by Vinnova (Sweden).